ESKİŞEHİR TECHNICAL UNIVERSITY JOURNAL OF SCIENCE AND TECHNOLOGY
A- APPLIED SCIENCES AND ENGINEERING

2019, 20(1), pp. 17 - 33, DOI: 10.18038/aubtda.474928

CHARACTERIZATION AND INVESTIGATION OF BIOLOGICAL PROPERTIES OF Ag-DOPED TiO_2 COATINGS FABRICATED ON TITANIUM

Salih DURDU *

Department of Industrial Engineering, Faculty of Engineering, Giresun University, Giresun, Turkey

ABSTRACT

In present study, Ag-doped TiO_2 bioceramic coatings are fabricated on cp-Ti by plasma electrolytic oxidation (PEO) and physical vapor deposition (PVD). The phase composition, surface microstructure, elemental composition, surface topography, wettability and chemical state of the PEO and Ag-doped TiO_2 surfaces are characterized by using powder- and thin film-X-ray diffraction (TF-XRD), scanning electron microscopy (SEM), energy dispersive spectroscopy (EDS), surface profilometer and contact angle measurement system (CAM), respectively. The PEO coating' surface is porous and rough due to the nature of process. The Ti, anatase-TiO_2, rutile-TiO_2 and Ag_2O phases are detected on the Ag-doped PEO surfaces by TF-XRD while The Ti, anatase and rutile phases are obtained on the PEO surfaces. The surface morphological structures of the PEO and Ag-doped PEO coatings are nearly identical although the surface chemistry of it is changed by PVD process. The Ti, O, P and Ag elements are observed on the Ag-doped PEO surfaces by EDS. Also, the amount of Ag existed on the surface is below cytotoxic limit. The Ag-doped PEO surfaces indicate better hydrophilic character to the PEO surface owing to increasing polarity of the surfaces. *In vitro* hydroxyapatite-forming ability is evaluated by immersion in simulated body fluid (SBF) at 36.5 °C for 28 days. The Ag-doped PEO surfaces show good hydroxyapatite formation ability compared to the PEO surface. The antibacterial activity is evaluated by exposing the samples to *Staphylococcus aureus* (*S. aureus*) and *Escherichia coli* (*E. coli*). And then, they are compared by the reaction of the pathogens to Ag-doped PEO with the PEO controls. The antibacterial ability of the Ag-doped PEO surfaces is significantly improved respect to the PEO surfaces for *S. aureus* and *E. coli*.

Keywords: Plasma electrolytic oxidation (PEO), Silver (Ag), Hydroxyapatite, Hydrophilic surface, *in vitro* properties

1. INTRODUCTION

Titanium and its alloys have light weight, high specific strength, great corrosion resistance and biocompatibility. So, they have preferred in the field of biomedical applications (e.g. artificial joints, dental and orthopedic implants) [1-3]. Especially, commercially pure titanium (cp-Ti) is widely used for dental implant applications [4, 5]. The passive protective oxide layer naturally forms on titanium. However, the passive layer on titanium cannot chemically and biologically bond to bone tissue due to its bioinert nature (low bioactivity). This directly prevents the adhesion of bone cells on titanium implant surface after the surgical implantation [6, 7]. Therefore, in order to enhance bioactivity, TiO_2 and/or hydroxyapatite-based bioceramic structures are coated on titanium implant surfaces by various surface modification techniques such as plasma spray [8-10], sol-gel [11, 12], acid etching [13] and sand blasting [14, 15]. Unfortunately, these techniques exhibit some limitations such as low adhesion, phase impurity and poor durability [1].

Plasma electrolytic oxidation (PEO), also known as micro arc oxidation (MAO), could be suggested versatile method for biologically enhancing the surface characteristics. The PEO produces bioactive and biocompatible ceramic coating on light metals such as titanium, magnesium and zirconium [16-19]. Also, the PEO is a relatively novel electrochemical surface treatment using a hybrid of conventional electrolysis and plasma arc discharge in an alkaline electrolyte solution under high voltage [20, 21]. The quality of the PEO coatings can be controlled by electrolyte, pH and electrical parameters (e.g. voltage, time and frequency). The PEO technique fabricates micro porous and highly adherent bioactive and biocompatible layers on Ti-based implant surfaces [22]. The other advantages

*Corresponding Author: durdusalih@gmail.com; salih.durdu@giresun.edu.tr
Received: 25.10.2018 Accepted: 08.03.2019

of PEO technique are its low cost, simplicity, producibility of complex compounds and formability of uniform coatings on complex geometries [23].

The PEO coatings on Ti-based implant surface are porous and rough. It has been stated that the PEO surfaces exposed to the oral cavity could be at a higher risk of bacterial accumulation [24]. Bacterial accumulation leads to begin bacterial infection under body conditions. This situation induces mucositis and/or peri-implantitis. Eventually, it resulted in destroying dental implants [25]. Therefore, in order to prevent initial adhesion of bacteria, antibacterial agents are presented on the implant surfaces. It is well known that Ag is an important antibacterial agent. Thus, it has got more attention for biomedical implant applications in recent years [26, 27].

The antibacterial properties of the TiO_2/calcium phosphate-based PEO coatings on cp-Ti are enhanced by using Ag. For this purpose, some literature studies have been conducted [28-32]. Song et al. fabricated silver- (or platinum-) containing tricalcium phosphate and hydroxyapatite-based calcium coatings on cp-Ti substrates. And then, *in vitro* antibacterial activity and *in vitro* cytotoxicity were evaluated in that work [28]. Jia et al. investigated the cytotoxic and antibacterial properties of the Ag nanoparticles containing TiO_2-based micro porous PEO coatings on Ti substrates [29]. Wang et al. evaluated the antibacterial and cytotoxic properties of the Ag nanoparticles containing TiO_2-based PEO coatings on Ti substrates [30]. Zhang et al. fabricated the Co-doped Ag nanoparticles containing TiO_2 coatings on Ti by PEO technique. And then, they investigated *in vitro* antimicrobial activities of them [31]. Teker Aydogan et al. produced the Ag-nanoparticles containing hydroxyapatite-based surface on Ti (Grade 4) by PEO process. The antibacterial (against *S. aureus*) and cell (SAOS-2) characteristics of Ag-nanoparticle-based surfaces were compared with base PEO surfaces [32]. In these studies, Ag-nanoparticles containing TiO_2/hydroxyapatite-based surfaces were fabricated. Antibacterial properties of the coatings were improved respect to the plain PEO surfaces. In terms of antibacterial properties, the obtained results are very attractive and promising for biomedical implant applications. However, *in vitro* apatite forming ability (bioactivity) of these surfaces has not been investigated yet. Moreover, there is no information about homogeneous distribution of antibacterial Ag nanoparticles on the PEO surface.

There are a few literature studies on the fabrication and investigation of antibacterial properties of the Ag-incorporated PEO coatings by using combined hybrid production processes [33-36]. Zhang et al. produced the Ag-incorporated PEO coatings by combined magnetron sputtering (MS) and plasma electrolytic oxidation (PEO). As a first step, the Ag target was deposited on Ti substrate by MS technique and an AgTi layer was fabricated on Ti substrate. And then, as a second step, Ag-incorporated TiO_2 layer was formed by PEO technique. And then, antibacterial properties of these surfaces was investigated [33, 34]. Durdu et al. fabricated the Ag-incorporated PEO coatings on Ti substrate by combined PVD and PEO. Initially, the Ag nano layer that had thickness of 25 nm was accumulated on Ti by TE technique. Following to TE process, as a second step, Ag-incorporated TiO_2 layer was fabricated in Na_2SiO_3 and KOH-based electrolyte by PEO technique. Also, *in vitro* properties of these surfaces were evaluated [35]. Zhang et al. produced the antibacterial TiO_2 coating incorporating silver nanoparticles by plasma electrolytic oxidation and ion implantation. Cell culture and microbial tests of these surfaces were carried out in that work [36]. In these studies, surface chemistry, morphology and wettability of both surfaces was changed compared to each other. Furthermore, the Ag was observed in- and/or near- micro discharge channels whereas the reported results are promising addressing the aforementioned problems such as antibacterial properties. Eventually, bacterial adhesion can be occurred on the surface regions except for micro discharge channel regions. However, it has not been clear bioactivity and antibacterial effects of Ag-deposited nano layer on TiO_2-based PEO bioceramic surfaces yet. There is no information about this work in literature. Thus, the fabrication, characterization and investigation of *in vitro* biological properties (e.g. bioactivity and antibacterial characteristics) of Ag-nano layer on bioceramic surfaces by combined PEO and PVD techniques were decided in this work.

The main objective of this work is to prepare an antibacterial and bioactive Ag-doped TiO_2 surfaces on cp-Ti substrates by combined PEO and PVD processes. Initially, a bioactive and biocompatible anatase and rutile-based TiO_2 bioceramic structures on cp-Ti substrate were coated by PEO technique in an alkaline electrolyte, consisting of Na_3PO_4 and KOH in deionized water. And then, an Ag nano layer had average thickness of 5 nm was deposited on the PEO coatings by PVD technique. The phase composition, surface microstructure, surface topography, elemental composition and wettability of the PEO and the Ag-doped PEO coatings were characterized by powder-XRD, TF-XRD, SEM, EDS, surface profilometer and CAM, respectively. And then, *in vitro* bioactivity under immersion in SBF for 28 days and *in vitro* microbial properties for gram positive (*S. aureus*) and gram negative (*E. coli*) bacteria was investigated in detail.

2. EXPERIMENTAL DETAILS

2.1. Sample Preparation at Pre-Coating Processes

Rectangular commercially pure titanium (cp-Ti) plates had the sizes of 65mm x 25mm x 5mm were used as substrate sample. All surfaces of the cp-Ti samples were abraded with SiC papers of 200, 400, 600, 800, and 1200 grit in turn, respectively. And then, they washed in an ultrasonic bath for 30min with deionized water and acetone. Eventually, the cp-Ti plates were dried in a stove at room temperature.

2.2. Plasma Electrolytic Oxidation (PEO)

The PEO process was carried out on cp-Ti plates by using an AC type high power supply (with maximum 100 kW). The cp-Ti substrate served as anode while a stainless steel container was used as cathode. The alkaline electrolyte consisted of sodium phosphate ($Na_3(PO_4)_2$) and potassium hydroxide (KOH) was prepared in deionized water. The PEO process was performed on a constant current mode in the 0.230 A/cm^2 for 10 min. And then, porous and rough bioceramic coatings were formed on cp-Ti surfaces. The temperature was below 30 °C by a water cooled chiller in a double wall container throughout the PEO. After the PEO was completed, the coatings were washed in deionized water. Afterwards, they dried in a stove at 35 °C for 24 h. All samples were protected in desiccators.

2.3. Physical Vapor Deposition (PVD)

An Ag nano layer (Alfa Aesar 99.99 % purity) was deposited on the PEO surfaces at 25 °C at pressure of $3x10^{-5}$ mbar in a vacuum-controlled thermal evaporation system by PVD (Vaksis 2T). The base pressure of vacuum-controlled chamber was about $1x10^{-7}$ mbar. Ag-powders were evaporated in a tungsten boat. And then, they were deposited on the PEO surfaces. Average thickness of Ag-nano layer was measured as about 5 nm by a quartz crystal thickness monitor (QCTM) attached to PVD device. The deposition rate was kept as 0.1 nm/s during PVD. The current was gradually increased up to 40 A. Eventually, the Ag were deposited onto the PEO surfaces. The photographs of all samples are shown in Figure 1.

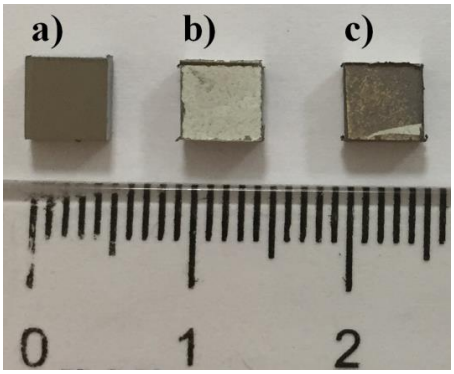

Figure 1. The photographs of the samples: a) cp-Ti substrates, b) the PEO coating and c) Ag-doped PEO coating

2.4. Characterization of the Surfaces

The phase compositions of the PEO and Ag-doped PEO surfaces were investigated by powder-XRD (Bruker D8 Advance) and TF-XRD (PANalytical X'Pert PRO MPD) with Cu-Kα radiation at a scanning speed of 0.1° min^{-1} from 20° to 90°, respectively. The surface microstructures and elemental compositions of both surfaces were analyzed by SEM (Philips XL30S FEG) and EDS at pre- and post-immersion in SBF *(in vitro* bioactivity tests), respectively. The 3-dimensional surface topography was evaluated by surface profilometer (KLA Tencor P-7). The surface profile values were achieved by a scanning area of 500μm x 500μm in 3-D. The average contact angles of the surfaces were measured for 60 s after the deionized water droplet with vol. of 1 μL was contacted onto the surfaces by using sessile drop technique CAM (Dataphysics OCA 15EC) system.

2.5. *In vitro* Bioactivity Tests of the Surfaces

The PEO and Ag-doped PEO coating samples were immersed at 36.5 °C in 1.0 X SBF. The SBF ion concentrations were nearly equal to those in human blood plasma. The SBF was prepared by dissolving reagent grade chemicals of NaCl, $NaHCO_3$, KCl, $K_2HPO_4.3H_2O$, $MgCl_2.6H_2O$, $CaCl_2$, and Na_2SO_4 in deionized water, respectively. And then, they buffered at pH 7.4 with $(CH_2OH)_3CNH_2$ (tris-hydroxymethyl-aminomethane) and 1.0-M hydrochloric acid (Titrisol®) at 36.5 °C [37]. SBF was refreshed through every 24 h. Thus, the ion concentration was maintained for 28 days. After immersion process was completed on 28 days, the samples were removed from the SBF. Then, they washed with deionized water and dried under room temperature. The phase compositions, surface morphology and elemental composition of both immersed surfaces were analyzed by TF-XRD. SEM and EDS, respectively.

2.6. *In vitro* Antibacterial Activity of the Surfaces

Antibacterial activities of the PEO and Ag-doped PEO surfaces were evaluated against Gram negative *E. coli* and Gram positive *S. aureus* by using colony counting method. The coating surfaces were immersed in 5.0 mL of the bacterial suspension ($1x10^7$ CFU/mL) and incubated for 24 h 37 °C. After incubation, all samples were washed with 150 mM NaCl. And then, each sample put into a tube containing 2 mL phosphate buffer solution and shaken on a vortex for 2 min to detach the bacteria from the surface into the solution. Aliquots of 100 μL of the solution were plated onto Muller Hinton Agar (MHA) plates, incubated at 37 °C for 48 h and then the active bacteria colonies were counted.
All characterization and *in vitro* experiments of the surfaces were carried out in triplicate.

3. RESULTS AND DISCUSSION

3.1. Powder-XRD Analysis of the PEO Coatings

The phase compositions of the PEO coating were analyzed by powder-XRD as shown in Figure 2. Titanium (JCPDS card number: 044-1294), anatase-TiO_2 (JCPDS card number: 21-1272) and rutile-TiO_2 (JCPDS card number: 21-1276) phases were detected on the PEO surface. In addition to the existence of Ti phase, mainly anatase and rutile were observed on the PEO surface. TiO_2 structure is continuously produced on the cp-Ti surface under high anodic potential through the PEO process by the electrochemical ionization reactions. An alkaline electrolyte contains Na^+, K^+, PO_4^{3-} and OH^- ions. After the PEO device starts, the Ti metal immersed into alkaline electrolyte ionized positively charged Ti^{4+} ions. Simultaneously, positively charged Ti^{4+} ions react with negatively charged OH^- ions because of the presence of opposite charges through the PEO. The opposite charged of Ti^{4+} and OH^- ions preferentially combine with each other. Eventually, porous and rough TiO_2 layer forms on the cp-Ti substrate. TiO_2 (titania) structure has three polymorph such as anatase, rutile and brookite. The rutile is thermodynamically more stable than the anatase. Primarily, metastable anatase forms at low

temperatures on the cp-Ti through the PEO process. And then, it transforms to stable rutile at high temperatures owing to high pressure and sintering effect inner layer of the coating at the next step of the PEO process. The phase transformation of anatase to rutile occurs during the PEO process. The anatase to rutile transformation is not instantaneous; it is time dependent since it is reconstructive [38]. All reactions through the PEO process are below:

Dissolution reactions in electrolyte:

$Na_3PO_4 \rightarrow Na+ + PO_4^{3-}$ Eq. 1

$KOH \rightarrow K^+ + OH^-$ Eq. 2

Cathodic reactions:

$2H_2O + 2e^- \rightarrow H_2 + 2OH^-$ Eq. 3

Anodic reactions:

$Ti \rightarrow Ti^{4+} + 4e^-$ Eq. 4

$Ti^{4+} + 4OH^- \rightarrow TiO_2 + 2H_2O$ Eq. 5

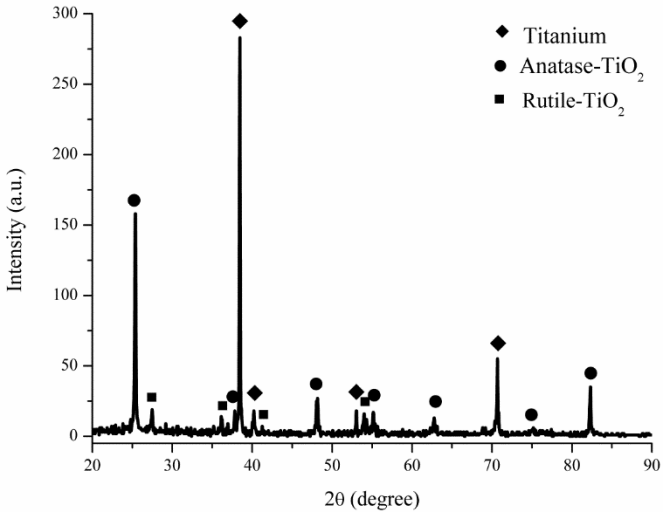

Figure 2. The powder-XRD spectra of the PEO coating

3.2. TF-XRD Analysis of the Ag-Doped PEO Coatings

The phase compositions of the Ag doped on the PEO surface were detected by TF-XRD as seen in Figure 3. The Ti (JCPDS card number: 04-004-8480), TiO_2 (JCPDS card number: 01-070-2556), anatase-TiO_2 (JCPDS card number: 01-083-5914), rutile-TiO_2 (JCPDS card number: 04-006-8034) and Ag_2O (JCPDS card number: 01-078-5867) phases were detected on the Ag-doped PEO surface. The TiO_2, anatase and rutile phases exist as the major phases while a trace amount of Ti and Ag_2O phases obtain on the Ag-doped PEO surface. An Ag layer has thickness of about 5nm is deposited onto the PEO surface under high vacuum conditions by PVD technique. The PEO layer on cp-Ti contains mainly oxide structures such as stable anatase- and rutile-TiO_2 at constant deposition temperatures. So, The Ag cannot react with stable oxide structures in PEO layer. Also, it maintains its metallic existence under vacuum conditions during PVD process. However, oxygen affinity of it is high to other IB elements such as Au and Cu. Thus, after the Ag-doped PEO surfaces remove the vacuum chamber, accumulated Ag atoms on the PEO surface combine with free oxygen gaseous (O_2) in air conditions. As a result of this, Ag deposited on the PEO surface reacts with O_2 gaseous in air at post-production process in PVD system and stable Ag_2O structure form on the PEO surface at post-production process in PVD. A trace amount of crystalline Ag_2O was detected by TF-XRD as seen in

Figure 3 surface since the amount of Ag-deposited on the PEO is low. The predicting formation mechanism of Ag_2O is below:

$$4Ag + O_2 \rightarrow 2Ag_2O \quad \text{Eq. 6}$$

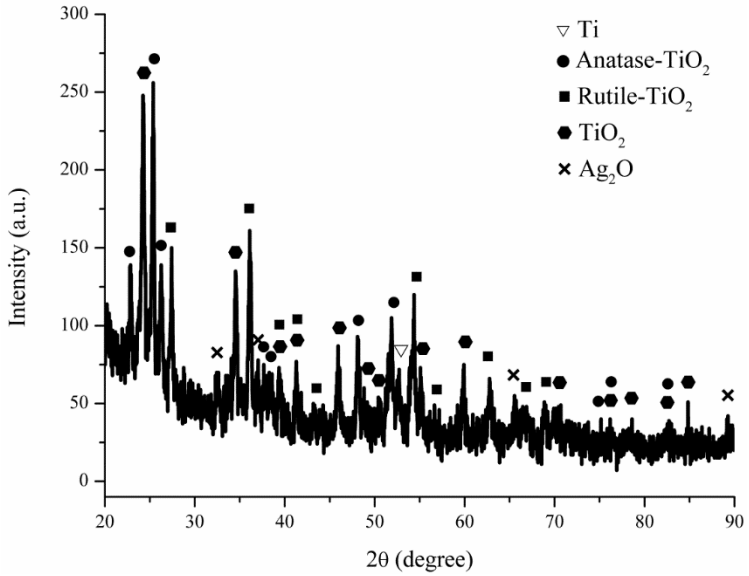

Figure 3. The TF-XRD spectra of the Ag-doped PEO coating

3.3. SEM Analysis of the Coatings

The surface microstructures of the PEO and Ag-doped PEO coatings were illustrated in Figure 4a and Figure 4b, respectively. As seen in Figure 4a and Figure 4b, there are many different-sized circular and spherical porous crater-like volcano structures on both surfaces. The micro sparks with high energy occur through the PEO process cause to form micro discharge channels on the metallic substrate. The high energy of micro sparks which provides local pressure and temperature of approximately 10^2 - 10^3 MPa and 10^3 - 10^4 K, respectively [39]. These values are high enough to give rise to plasma thermochemical interactions between cp-Ti substrate and alkaline electrolyte. The melt-quenched high-temperature complex oxide compounds on cp-Ti substrate surface formed by these plasma thermochemical interactions. The complex oxide compounds contain both the substrate material and electrolyte-borne modifying elements [21]. It is evident that the PEO surfaces contain distributed dark circular and spherical spots. These structures are called as micro discharge channels. The local higher temperature occurred in micro discharge channels, the short discharge lifetime and high cooling rate during PEO reduce the effective temperature of film synthesis [40]. However, high temperature values occurred through the PEO process is greater than sintering temperatures of anatase and rutile-based oxide structures on cp-Ti substrate. The micro discharge channels make contact between cp-Ti and the bioceramic coating due to open structure. So, the existence of porous surface structure is interested with the micro discharge channels. However, the surface morphology of the PEO coatings does not change by PVD process. In previous study, the surface morphology of the PEO coatings on Ag-deposited Ti substrates produced by PVD process were considerably changed compared to the PEO coatings on cp-Ti substrates [35]. Similarly, in another study, the surface microstructures of plain PEO and the PEO coatings on AgTi layers fabricated by PVD-MS (magnetron sputtering) technique were different from each other [33, 34]. However, in this study, the porous and rough surface of the Ag-doped PEO coating are maintained because the Ag layer was deposited on the PEO surfaces at nanometer scale. This is beneficial for the apatite formation as seen Figure 7. In addition to Figure 4, the surfaces of them are very rough as seen in Figure 5.

a)

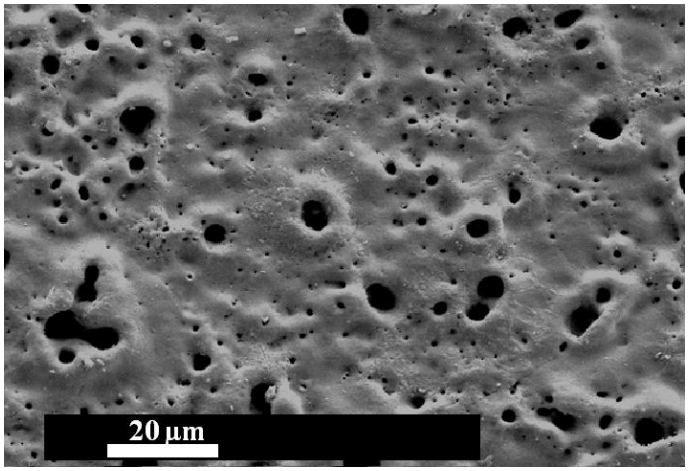

b)

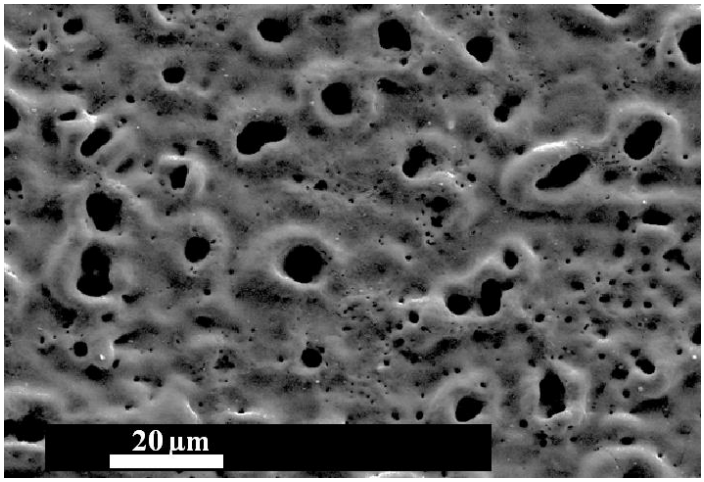

Figure 4. Surface morphologies of both coatings: a) the PEO coating and b) Ag-doped PEO coating

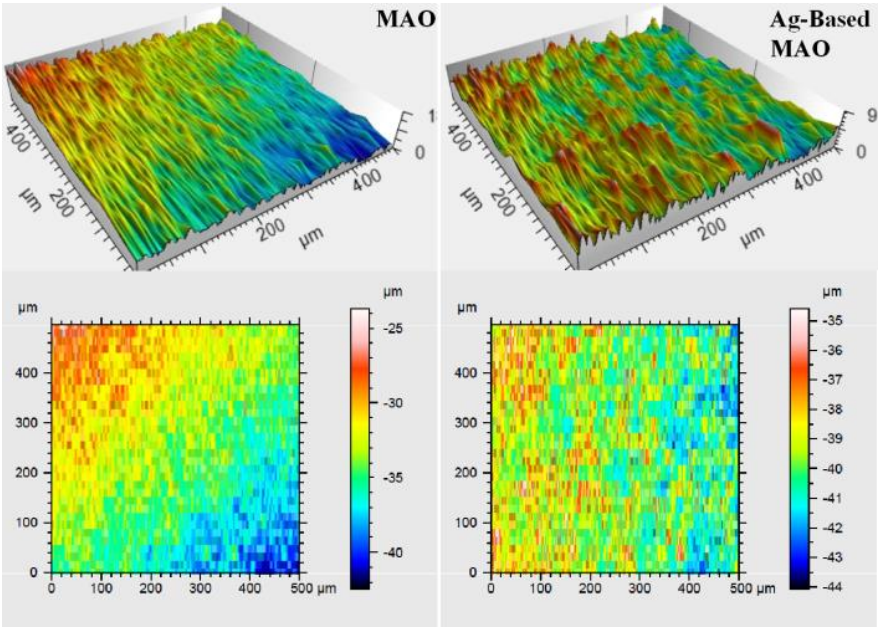

Figure 5. Surface topographies of the coatings: a) the PEO coating and b) Ag-doped PEO coating

3.4. EDS Analysis of the Coatings

The elemental amount on the PEO and Ag-doped PEO surfaces were determined by EDS as given in Table 1. Additional Ag element was observed on the Ag-doped PEO surface as the Ti, O and P elements were detected on both surfaces. A high amount of Ti and O elements obtained on both surfaces as supported in Figure 2 and Figure 3. The presences of them originate from the cp-Ti substrate and TiO_2-based surface. However, both coating structures have low amount of P element. Also, elemental or compound P structure could not be detected on the surfaces by powder- and TF-XRD whereas the coatings contain elemental P element as seen in Table 1. The P element comes from anionic PO_4^{3-} ions in alkaline electrolyte. The anionic PO_4^{3-} ions can react with cationic Ti^{4+} ions through the PEO process due to the electrostatic interactions of opposite charges. However, reaction products could not transform to crystalline form since they could not be detected by powder- / TF-XRD as shown in Figures 1 and 2. Therefore, it can be stated that the elemental / compounds P structures are found amorphous form on the surfaces. Moreover, a trace amount of Ag was observed on the Ag-doped PEO surface. This arises from the deposition of Ag on the PEO surface. The amount of Ag is below cytotoxic limit as reported in literature [41].

Table 1. EDS spectra results of the PEO and Ag-doped PEO coatings.

Elements	The PEO coating			Ag-doped PEO coating		
	Weight %	Atomic %	Net Error	Weight %	Atomic %	Net Error
O	30.53	54.87	0.01	41.90	67.17	0.01
P	10.44	9.70	0	7.29	6.04	0
Ti	59.03	35.43	0	49.43	26.47	0
Ag	-	-	-	1.38	0.33	0.15

3.5. Wetting test of the Coatings

To evaluate wettability (hydrophilicity / hydrophobicity) of the both different surfaces, the contact angle measurement analysis was carried out as illustrated in Figure 6. Average contact angles of the PEO and Ag-doped PEO coatings were obtained as about 95.6° and 90.4°, respectively. The both surfaces are porous and rough as seen in Figure 4. The porous coating surfaces exhibit hydrophilic properties owing to the capillary effect on the liquid of pores [42]. Furthermore, the Ag-doped PEO coatings had more hydrophilic character than the PEO coatings. The surface wettability is affected from some parameters such as morphology, crystallinity and chemistry [43, 44]. It is clear that the hydrophilicity of the Ag-doped PEO surfaces is better than the one of plain PEO surfaces whereas the surface morphologies of them are nearly identical. However, the surface chemistry of them is different from each other. Therefore, it can be stated that the Ag-layer deposited on the PEO surfaces improve the surface wettability because it contributes to enhance the surface polarity compared to the plain PEO surfaces. Moreover, the surface wettability (hydrophilicity) is vitally important for the adsorption of proteins and the cell adhesion. It gives predicting information about *in vitro* bioactivity. Thus, according to these, Ag-doped PEO surface is beneficial for *in vitro* bioactivity as observed in Figure 7 and Figure 8.

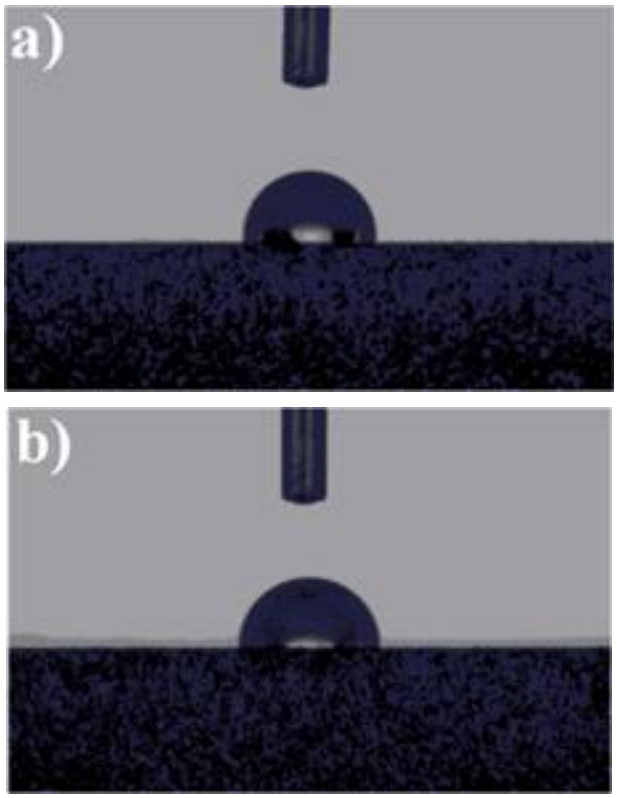

Figure 6. The contact angle images on both coating surfaces at 60th s after droplet contacting: a) the PEO coating and Ag-doped PEO coating surfaces.

3.6. *In vitro* Apatite Forming Ability of the Coatings

The apatite forming ability on the implant materials gives predicting information about *in vitro* bioactivity. Therefore, apatite forming ability on the immersed implant materials in SBF under *in vitro* body conditions is an essential assessment to be prescient about bioactivity. However, "Apatite-forming ability is just a necessary but by no means sufficient precondition of 'bioactivity'. 'Bioactivity' is a very complex interplay of many factors, where apatite-forming ability is just one of many" [45]. After immersion tests were completed at 36.5 °C for 28 days, the phase compositions of the PEO and Ag-doped PEO coating surfaces were investigated by TF-XRD as shown in Figure 7. The phases of Ti (JCPDS card number: 04-004-8480), anatase (JCPDS card number: 01-083-5914), rutile (JCPDS card number: 04-006-8034), TiO_2 (JCPDS card number: 01-070-2556), $Ca_3(PO_4)_2$ (TCP: JCPDS card number: 044-1294) and $Ca_{10}(PO_4)_6(OH)_2$ (hydroxyapatite-HA: JCPDS card number: 00-009-0432) were detected on the PEO and Ag-doped PEO coatings surfaces at post-immersion in SBF. The phases of Ti, TiO_2, anatase and rutile have already existed in both coating structures. Also, the phases of TCP and HA are observed because positively charged Ca^{2+} and negatively charged PO_4^{3-} ions in SBF solution were diffused and reacted on Ti-OH-based original surface. It is well known that TiO_2 structure is a positively charged oxides [46]. Positively charged surfaces promote cell adhesion as negatively charged surfaces reduce it [47]. Therefore, the OH^- groups on TiO_2 surfaces dissociate to give positive charges, favoring cell attachment and proliferation [48, 49]. The positively charged Ca^{2+} and negatively charged PO_4^{3-} ions diffuse onto free OH^- groups in TiO_2-based surfaces in turn due to the electrostatic interactions in SBF through immersion process. Simultaneously, they reacted with each other produced during immersion process. And then, the phases of TCP and HA forms on TiO_2-based surfaces. The Ca^{2+} and PO_4^{3-} ions combine under SBF conditions after they diffuse onto TiO_2-based surface. The TCP was formed by the reacting of Ca^{2+} and PO_4^{3-} ions. Simultaneously, Ca^{2+}, PO_4^{3-} and OH^- ions combine with each other and they form the HA structure on both surfaces. The HA

nuclei spontaneously grow at the expense of calcium and phosphate ions from the metastable supersaturated SBF solution as they are formed. It is suggested that the crystallinity of apatite can be controlled by immersion time in the SBF. As seen in Figure 7, the amount and intensity of crystalline hydroxyapatite formed on the Ag-doped PEO surfaces are greater than ones of the PEO surfaces. The formation mechanism of HA on both surfaces during immersion in SBF are below:

$$10Ca^{2+} + 6PO_4^{3-} + 2OH^- \rightarrow Ca_{10}(PO_4)_6(OH)_2 \qquad \text{Eq. 6}$$

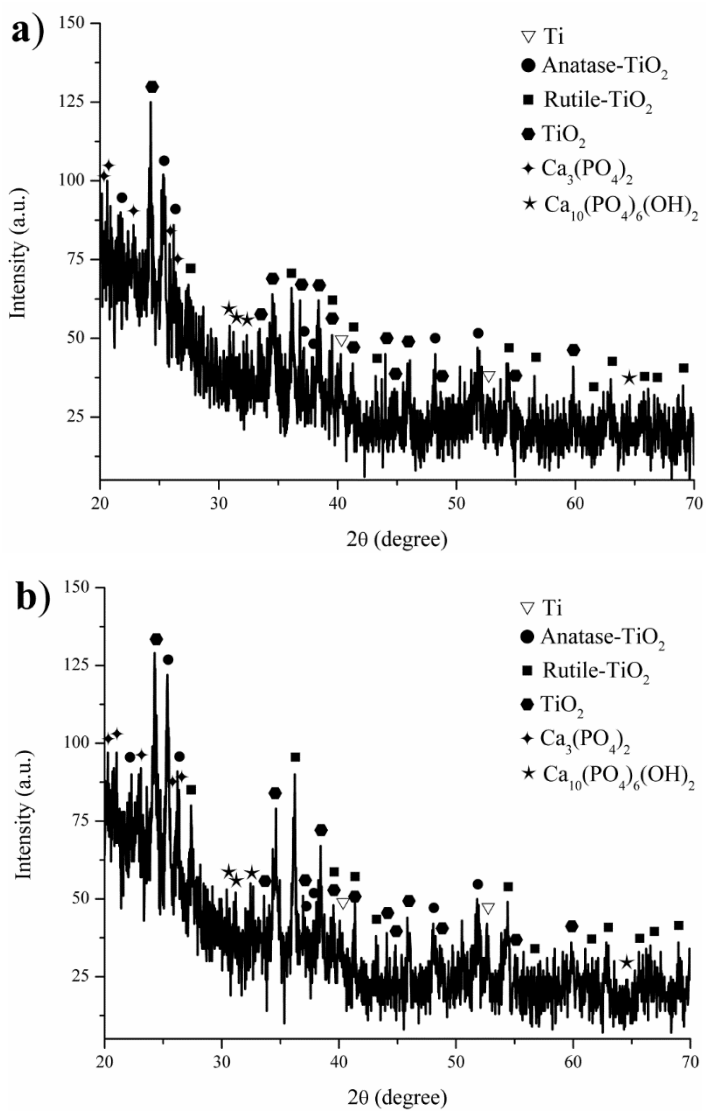

Figure 7. TF-XRD spectra pattern of the coatings at post-immersion in SBF at 36.5 °C for 28 days: a) the PEO coating and b) Ag-doped PEO coating.

After immersion tests were completed at 36.5 °C for 28 days, the surface morphology of both surfaces was characterized by SEM as given in Figure 8. Newly fine dispersed HA structures separately formed on both surfaces as supported in Figure 7a and Figure 7b. Fine dispersed HA structures at post-immersion process were not stratified and not completely covered at non-porous regions on both surfaces. However, they covered and filled into porous surfaces as seen in Figure 8. Also, the HA layer formed on Ag-doped PEO is more homogeneous and denser than one on the PEO surface (Figure 8c and Figure 8d) as supported in Figure 7.

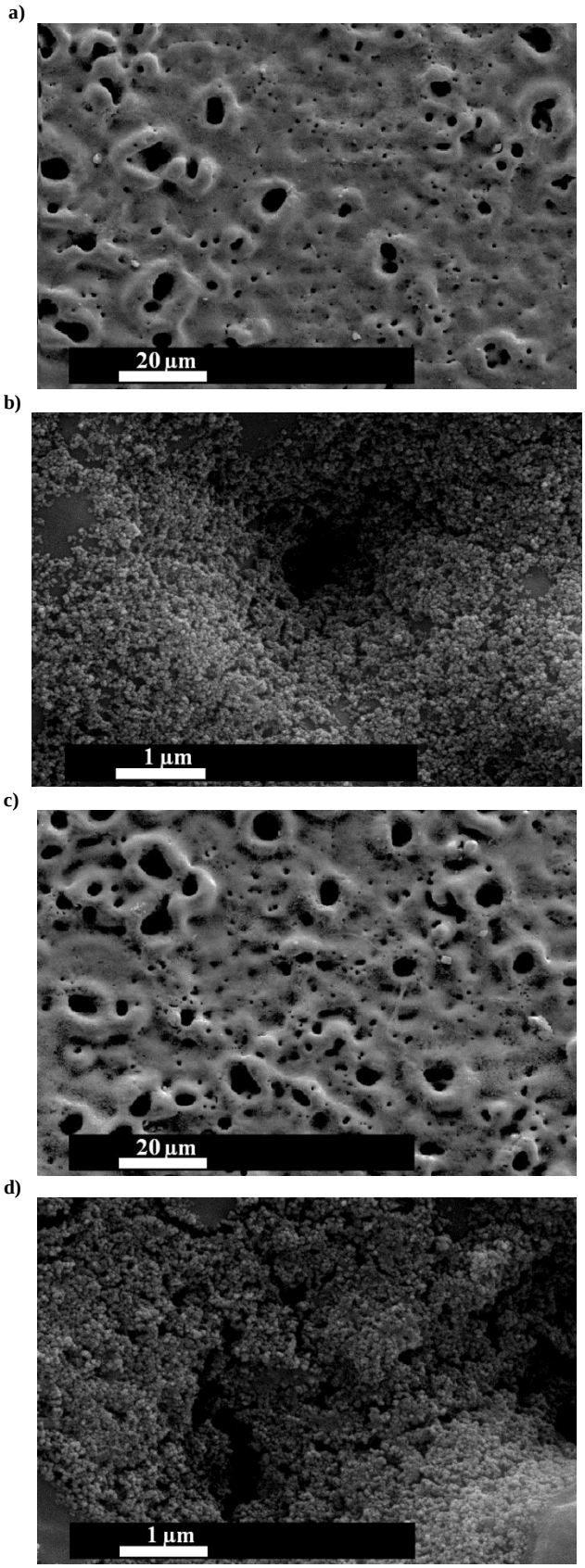

Figure 8. Surface morphologies of both coatings at post-immersion in SBF at 36.5 °C for 28 days: a) and b) the PEO coating and c) and d) the Ag-doped PEO coating.

The elemental amount on the PEO and Ag-doped PEO surfaces were determined by EDS as shown in Table 2. The Ti, O and P elements were obtained on both surfaces at post-immersion in SBF as expected. Also, a trace amount of Ag was observed on the Ag-doped PEO surface. However, the amount of it acquired in Table 2 is very low compared to one in Table 1 because the Ca and P covered on both surfaces. Furthermore, the Ca and P elements, originate from SBF solution, were deposited on both surfaces through the immersion process. The presence of Ag on the PEO surface accelerates the Ca and P deposition rate under the same immersion conditions as shown in Figures. 7 and 8. As seen in Table 2, the amounts of Ca and P accumulated on the Ag-doped surface are greater than ones on the PEO surface at post-immersion process. According to these data, it can be clearly stated that Ag nano layer on the TiO_2-based surfaces triggers the apatite formation under immersion in SBF conditions. Thus, it could be stated that the existence of Ag elements on the PEO surfaces improves *in vitro* bioactivity / apatite-forming ability.

Table 2. EDS spectra results of the PEO and Ag-doped PEO coatings at post-immersion in SBF at 36.5 °C for 28 days.

Elements	The PEO coating			Ag-doped PEO coating		
	Weight %	Atomic %	Net Error	Weight %	Atomic %	Net Error
O	35.04	60.13	0.01	38.56	63.22	0.01
P	8.14	7.22	0.01	10.24	8.67	0
Ca	0.77	0.53	0.13	1.14	0.74	0.07
Ti	56.05	32.13	0	49.91	27.33	0
Ag	-	-	-	0.15	0.04	0.36

3.7. *In vitro* Antibacterial Properties of the Coatings

To determine the antibacterial activity of the PEO and Ag-doped PEO surfaces, the adhered bacteria to surfaces were removed and re-cultivated for colony counting. Figure 9 shows the antibacterial activity of both surfaces against gram-positive (*S. aureus*) and gram-negative (*E. coli*) bacteria. It was observed that the antibacterial property was significantly changed on Ag nano layer (Ag_2O) on the PEO surface compared to plain PEO surface. The antibacterial activity of the Ag-doped PEO surfaces against *E. coli* and *S. aureus* was determined as 71.0 % and 68.2 %, respectively. Liu et al. reported that antibacterial properties of TiO_2/Ag_2O heterostructure composites are greater than pure TiO_2 for *E. coli* bacteria type [50].

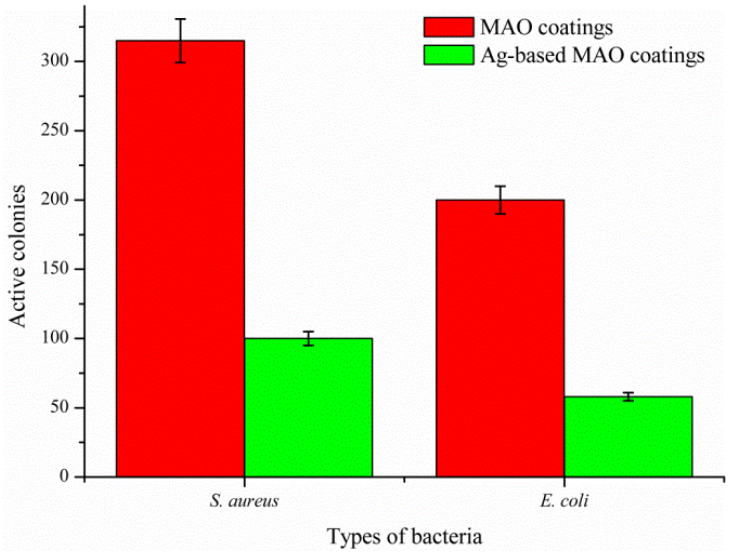

Figure 9. Active colony ratios of *S. aureus* as gram positive bacteria and *E. coli* as gram negative bacteria on the coatings: a) the PEO coatings and b) Ag-doped PEO coatings after re-cultivation.

The Ag-doped PEO surfaces reveal some important points. One of these is that the deposition of Ag_2O increases antibacterial property of surfaces as seen in Figure 9. Ag_2O have great antimicrobial activity. It is believed that metal oxide nanoparticles such as Ag_2O might be considered as a novel alternative to the most antibiotics [51]. It is well known that Ag^+ ions which are toxic can kill the bacteria through the denaturation or oxidation mechanism. Solid oxidized silver states such as Ag_2O should be a candidate source to replace the Ag^+ solution since they are able to produce a more sustained release of Ag^+ ions [52]. So, the increase in the antibacterial activity of Ag-doped PEO surfaces can be explained by the toxic effects of Ag^+ ions on bacteria cell. The protein molecules, enzymes and transporters on the cell surface become denatured at post-interaction of the Ag ions with the bacteria cell. And then, the intracellular signal pathway and DNA synthesis are blocked [53, 54]. In addition, the electrostatic interaction between positively charged Ag ions and negatively charged bacterial cells leads to degradation of cell membrane integrity and bactericidal effect [55]. As a consequence of these effects on the bacterial cell, the cell cycle is disrupted and proliferation is reduced. These lead to decrease in colony formation. Similarly, Zhang et al. reported that Ag incorporated coatings present strong inhibition against *S. aureus* compared to plain control coatings [36].

The plate images for *S. aureus* and *E. coli* of the PEO and Ag-doped PEO surfaces' cultivations were given in Figure 10 and Figure 11, respectively. The antibacterial properties of the surfaces varied according to the bacterial species tested in this study. Ag-doped PEO surfaces show a higher antibacterial activity against *E. coli* compared to *S. aureus*. The antibacterial activity of Ag-doped PEO coatings against *E. coli* is 1.72 times higher than that of the *S. aureus*. This result can be explained by the cellular differences between gram-positive and gram-negative bacteria. The thick peptidoglycan layer in *S. aureus* prevents transportation of Ag ions across the bacterial cell wall. Moreover, it reduces the toxic effects of Ag [53]. This is also supported by similar studies at literature studies. Feng et al. reported that was *S. aureus* was less affected than *E. coli* on Ag toxicity. Also, the different bacteria types were associated with the structural properties of cells [53].

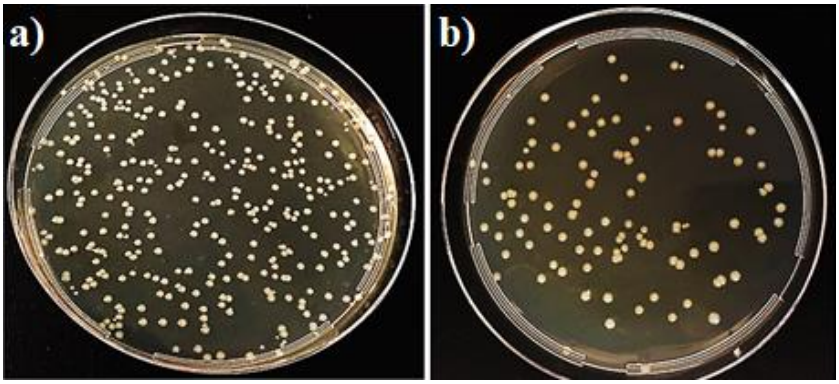

Figure 10. Culture plate photographs of *S. aureus* after re-cultivation: a) the PEO and b) Ag-doped PEO surface cultivation.

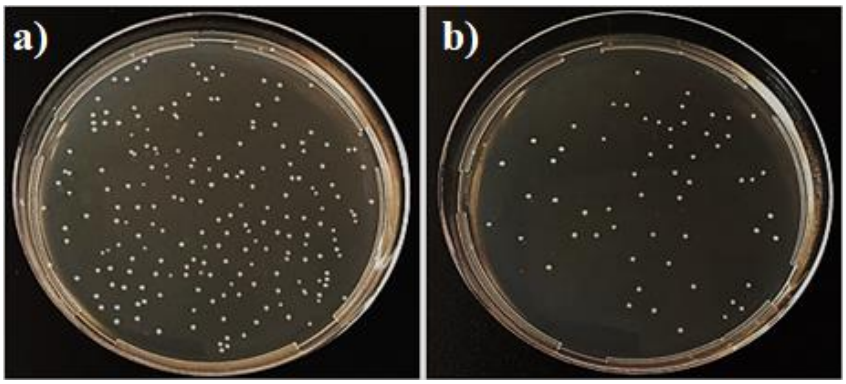

Figure 11. Culture plate photographs of *E. coli* after re-cultivation: a) the PEO and b) Ag-doped PEO surface cultivation.

4. CONCLUSION

In summary, Ag-doped TiO_2-based surfaces, contained antibacterial, bioactive and biocompatible elements were fabricated on cp-Ti by PEO and PVD techniques. The Ag, Ti, O and P were observed through the whole surfaces. The Ag-doped PEO surface indicated hydrophilic character respect to plain PEO surface whereas the surface morphology of them was not changed by PVD. *In vitro* bioactivity and apatite-forming abilities of the Ag-doped PEO surfaces were considerably improved to the PEO surfaces as seen in TF-XRD, SEM and EDS results. Moreover, antibacterial properties of the Ag-doped PEO surfaces were greater than ones of the PEO surface for *S. aureus* and *E. coli*. Therefore, the Ag-doped porous TiO_2-based coatings can be potential candidate for implant surface modification applications owing to their promising antibacterial and bioactive properties.

ACKNOWLEDGEMENTS

The author would like to special thank Mr. F. Unal for running Physical Vapor Deposition Thermal Evaporation System at Giresun University GRUMLAB, Mr. A. Nazim for running SEM and EDS, Mr. A. Sen for running powder-XRD at Gebze Technical University and Dr. Y. Ozturk for running TF-XRD at TUBITAK MAM Materials Institute.
This work was not supported by any funding organization. The author declares no conflict of interest.

REFERENCES

[1] Shin KR, Kim YS, Yang HW, Ko YG, Shin DH. In vitro biological response to the oxide layer in pure titanium formed at different current densities by plasma electrolytic oxidation. Appl. Surf. Sci. 2014; 314:221-227.

[2] Necula BS, Apachitei I, Fratila-Apachitei LE, van Langelaan EJ, Duszczyk J. Titanium bone implants with superimposed micro/nano-scale porosity and antibacterial capability. Appl. Surf. Sci. 2013; 273:310-314.

[3] Geetha M, Singh AK, Asokamani R, Gogia AK. Ti based biomaterials, the ultimate choice for orthopaedic implants - A review. Prog. Mater. Sci. 2009; 54(3):397-425.

[4] Osman RB, Swain MV. A Critical Review of Dental Implant Materials with an Emphasis on Titanium versus Zirconia. Materials 2015; 8(3):932-958.

[5] Le Guéhennec L, Soueidan A, Layrolle P, Amouriq Y. Surface treatments of titanium dental implants for rapid osseointegration. Dental Mater. 2007; 23(7):844-854.

[6] Niinomi M. Biologically and Mechanically Biocompatible Titanium Alloys. Mater. Transac. 2008; 49(10):2170-2178.

[7] Jones FH. Teeth and bones: applications of surface science to dental materials and related biomaterials. Surf. Sci. Rep. 2001; 42(3-5):79-205.

[8] Degroot K, Geesink R, Klein C, Serekian P. Plasma Sprayed Coatings of Hydroxyapatite J. Biomed. Mater. Res. 1987; 21(12):1375-1381.

[9] Lu YP, Li MS, Li ST, Wang ZG, Zhu RF. Plasma-sprayed hydroxyapatite plus titania composite bond coat for hydroxyapatite coating on titanium substrate. Biomaterials 2004; 25(18):4393-4403.

[10] Wang H-d, He P-f, Ma G-z, Xu B-s, Xing Z-g, Chen S-y, Liu Z, Wang Y-w. Tribological behavior of plasma sprayed carbon nanotubes reinforced TiO2 coatings. J. Europ. Cer. Soc. 2018; 38(10):3660-3672.

[11] Sidane D, Rammal H, Beljebbar A, Gangloff SC, Chicot D, Velard F, Khireddine H, Montagne A, Kerdjoudj H. Biocompatibility of sol-gel hydroxyapatite-titania composite and bilayer coatings. Mater. Sci. Eng. C 2017; 72:650-658.

[12] Horkavcová D, Novák P, Fialová I, Černý M, Jablonská E, Lipov J, Ruml T, Helebrant A. Titania sol-gel coatings containing silver on newly developed TiSi alloys and their antibacterial effect. Mater. Sci. Eng. C 2017; 76:25-30.

[13] Hazra SK, Tripathy SR, Alessandri I, Depero LE, Basu S. Characterizations of porous titania thin films produced by electrochemical etching. Mater. Sci. Eng. B 2006; 131(1):135-141.

[14. Farrokhi-Rad M. Electrophoretic deposition of fiber hydroxyapatite/titania nanocomposite coatings. Cer. Inter. 2018; 44(1):622-630.

[15] Farrokhi-Rad M. Electrophoretic deposition of titania nanostructured coatings with different porous patterns. Cer. Inter. 2018; 44(13):15346-15355.

[16] Duarte LT, Bolfarini C, Biaggio SR, Rocha-Filho RC, Nascente PAP. Growth of aluminum-free porous oxide layers on titanium and its alloys Ti-6Al-4V and Ti-6Al-7Nb by micro-arc oxidation. Mater. Sci. Eng. C 2014; 41:343-348.

[17] Kazek-Kęsik A, Krok-Borkowicz M, Pamuła E, Simka W. Electrochemical and biological characterization of coatings formed on Ti–15Mo alloy by plasma electrolytic oxidation. Mater. Sci. Eng. C 2014; 43:172-181.

[18] Echeverry-Rendon M, Duque V, Quintero D, Harmsen MC, Echeverria F. Novel coatings obtained by plasma electrolytic oxidation to improve the corrosion resistance of magnesium-based biodegradable implants. Surf. Coat. Technol. 2018; 354:28-37.

[19] Matykina E, Arrabal R, Skeldon P, Thompson GE, Wang P, Wood P. Plasma electrolytic oxidation of a zirconium alloy under AC conditions. Surf. Coat. Technol. 2010; 204(14):2142-2151.

[20] Yerokhin L, Snizhko LO, Gurevina NL, Leyland A, Pilkington A, Matthews A. Discharge characterization in plasma electrolytic oxidation of aluminium. J. Phy. D-Appl. Phy. 2003; 36(17):2110-2120.

[21] Yerokhin AL, Nie X, Leyland A, Matthews A. Characterisation of oxide films produced by plasma electrolytic oxidation of a Ti–6Al–4V alloy. Surf. Coat. Technol. 2000; 130(2–3):195-206.

[22] Adeleke SA, Ramesh S, Bushroa AR, Ching YC, Sopyan I, Maleque MA, Krishnasamy S, Chandran H, Misran H, Sutharsini U. The properties of hydroxyapatite ceramic coatings produced by plasma electrolytic oxidation. Cer. Int. 2018; 44(2):1802-1811.

[23] Sandhyarani M, Rameshbabu N, Venkateswarlu K, Krishna LR. Fabrication, characterization and in-vitro evaluation of nanostructured zirconia/hydroxyapatite composite film on zirconium. Surf. Coat. Technol. 2014; 238:58-67.

[24] Kotharu V, Nagumothu R, Arumugam CB, Veerappan M, Sankaran S, Davoodbasha M, Nooruddin T. Fabrication of corrosion resistant, bioactive and antibacterial silver substituted hydroxyapatite/titania composite coating on Cp Ti. Cer. Int. 2012; 38(1):731-740.

[25] Berglundh T, Persson L, Klinge B. A systematic review of the incidence of biological and technical complications in implant dentistry reported in prospective longitudinal studies of at least 5 years. J. Clin. Periodontol. 2002; 29:197-212.

[26] Hardes J, Ahrens H, Gebert C, Streitbuerger A, Buerger H, Erren M, Gunsel A, Wedemeyer C, Saxler G, Winkelmann W and others. Lack of toxicological side-effects in silver-coated megaprostheses in humans. Biomaterials 2007; 28(18):2869-2875.

[27] Chen L, Zheng L, Lv Y, Liu H, Wang G, Ren N, Liu D, Wang J, Boughton RI. Chemical assembly of silver nanoparticles on stainless steel for antimicrobial applications. Surf. Coat. Technol. 2010; 204(23):3871-3875.

[28] Song WH, Ryu HS, Hong SH. Antibacterial properties of Ag (or Pt)-containing calcium phosphate coating formed by micro-arc oxidation. J. Biomed. Mater. Res. A 2009; 88A(1):246-254.

[29] Jia ZJ, Xiu P, Li M, Xu XC, Shi YY, Cheng Y, Wei SC, Zheng YF, Xi TF, Cai H and others. Bioinspired anchoring AgNPs onto micro-nanoporous TiO_2 orthopedic coatings: Trap-killing of bacteria, surface-regulated osteoblast functions and host responses. Biomaterials 2016; 75:203-222.

[30] Wang JX, Li JH, Guo GY, Wang QJ, Tang J, Zhao YC, Qin H, Wahafu T, Shen H, Liu XY and others. Silver-nanoparticles-modified biomaterial surface resistant to staphylococcus: new insight into the antimicrobial action of silver. Sci. Rep. 2016; 6.

[31] Zhang L, Gao Q, Han Y. Zn and Ag Co-doped Anti-microbial TiO2 Coatings on Ti by Micro-arc Oxidation. J. Mater. Sci. Technol. 2016; 32(9):919-924.

[32] Aydogan DT, Muhaffel F, Kilic MM, Acar OK, Cempura G, Baydogan M, Karaguler NG, Kose GT, Czyrska-Filemonowicz A, Cimenoglu H. Optimisation of micro-arc oxidation electrolyte for fabrication of antibacterial coating on titanium. Mater. Technol. 2018; 33(2):119-126.

[33] Zhang X, Wu H, Geng Z, Huang X, Hang R, Ma Y, Yao X, Tang B. Microstructure and cytotoxicity evaluation of duplex-treated silver-containing antibacterial TiO_2 coatings. Mater. Sci. Eng. C 2014; 45:402-410.

[34] Zhang XY, Hang RQ, Wu HB, Huang XB, Ma Y, Lin NM, Yao XH, Tian LH, Tang B. Synthesis and antibacterial property of Ag-containing TiO_2 coatings by combining magnetron sputtering with micro-arc oxidation. Surf. Coat. Technol. 2013; 235:748-754.

[35] Durdu S, Aktug SL, Korkmaz K, Yalcin E, Aktas S. Fabrication, characterization and in vitro properties of silver-incorporated TiO_2 coatings on titanium by thermal evaporation and micro-arc oxidation. Surf. Coat. Technol. 2018; 352:600-608.

[36] Zhang P, Zhang ZG, Li W. Antibacterial TiO2 Coating Incorporating Silver Nanoparticles by Microarc Oxidation and Ion Implantation. J. Nanomater. 2013; 2013:1-8.

[37] Kokubo T, Takadama H. How useful is SBF in predicting in vivo bone bioactivity? Biomaterials 2006; 27(15):2907-2915.

[38] Hanaor DAH, Sorrell CC, Review of the anatase to rutile phase transformation, J. Mater. Sci. 2011; 46:855-874.

[39] Erfanifar E, Aliofkhazraei M, Nabavi HF, Sharifi H, Rouhaghdam AS. Growth kinetics and morphology of plasma electrolytic oxidation coating on aluminum. Mater. Chem. Phy. 2017; 185:162-175.

[40] Siegel RW, Ramasamy S, Hahn H, Li ZQ, Lu T, Gronsky R. Synthesis, characterization, and properties of nanophase TIO2. J. Mater. Res. 1988;3:1367-1372.

[41] Teker D, Muhaffel F, Menekse M, Karaguler NG, Baydogan M, Cimenoglu H. Characteristics of multi-layer coating formed on commercially pure titanium for biomedical applications. Mater. Sci. Eng. C 2015; 48:579-585.

[42] Zhang F, Chen S, Dong L, Lei Y, Liu T, Yin Y. Preparation of superhydrophobic films on titanium as effective corrosion barriers. Appl. Surf. Sci. 2011; 257(7):2587-2591.

[43] Planell JA, Navarro M, Altankov G, Aparicio C, Engel E, Gil J, et al. Materials Surface Effects on Biological Interactions. In: In V. P. Shastri GA, & A. Lendlein, (Eds.), editors. Advances in Regenerative Medicine: Role of Nanotechnology, and Engineering Principles: Springer; 2010. p 233-252.

[44] Meiron TS, Marmur A, Saguy IS. Contact angle measurement on rough surfaces. J. Coll. Interface Sci. 2004; 274(2):637-644.

[45] Kokubo T. Bioactive glass ceramics: properties and applications. Biomaterials 1991; 12(2):155-163.

[46] Fukuzaki S, Urano H, Nagata K. Adsorption of bovine serum albumin onto metal oxide surfaces. J. Ferm. Bioeng. 1996; 81(2):163-167.

[47] Bongrand P, Capo C, Depieds R. Physics of cell adhesion. Prog. Surf. Sci. 1982;12(3):217-285.

[48] Feng B, Weng J, Yang BC, Qu SX, Zhang XD. Characterization of surface oxide films on titanium and adhesion of osteoblast. Biomaterials 2003; 24(25):4663-4670.

[49] Zeng Q, Chen ZQ, Li QL, Li G, Darvell BW. Surface modification of titanium implant and in vitro biocompatibility evaluation. Key Eng. Mater. 2005; 288-289:315-318.

[50] Liu BK, Mu LL, Han B, Zhang JT, Shi HZ. Fabrication of TiO2/Ag2O heterostructure with enhanced photocatalytic and antibacterial activities under visible light irradiation. Appl. Surf. Sci. 2017; 396:1596-1603.

[51] Dizaj SM, Lotfipour F, Barzegar-Jalali M, Zarrintan MH, Adibkia K. Antimicrobial activity of the metals and metal oxide nanoparticles. Mater. Sci. Eng. C. 2014; 44:278-284.

[52] Wang X, Wu HF, Kuang Q, Huang RB, Xie ZX, Zheng LS. Shape-Dependent Antibacterial Activities of Ag2O Polyhedral Particles. Langmuir. 2010; 26:2774-2778.

[53] Feng QL, Wu J, Chen GQ, Cui FZ, Kim TN, Kim JO. A mechanistic study of the antibacterial effect of silver ions on Escherichia coli and Staphylococcus aureus. J. Biomed. Mater. Res. 2000; 52(4):662-668.

[54] Sondi I, Salopek-Sondi B. Silver nanoparticles as antimicrobial agent: a case study on E-coli as a model for Gram-negative bacteria. J. Coll. Interface Sci. 2004; 275(1):177-182.

[55] Stoimenov PK, Klinger RL, Marchin GL, Klabunde KJ. Metal oxide nanoparticles as bactericidal agents. Langmuir 2002; 18(17):6679-6686.